Supporting Information

Influence of Aromatic π-extension on Phenanthro[9,10-d]imidazole-based Donor-Acceptor Systems for Non-volatile Resistive *WORM* Memory Device Applications

Ajay Namitha,[a] Madanan Akshaya,[a] Predhanekar Mohamed Imran,[b] Nattamai. S. P. Bhuvanesh [c] and Samuthira Nagarajan,[, a]*

[a]*Division of Organic Electronics,* Department of Chemistry,
Central University of Tamil Nadu, Thiruvarur- 610 005, India
snagarajan@cutn.ac.in
[b]Department of Chemistry, Islamiah College, Vaniyambadi - 635 752, India
[c]Department of Chemistry, Texas A &M University, TX77842, USA

Table of contents

1. Synthesis and spectral data of compounds

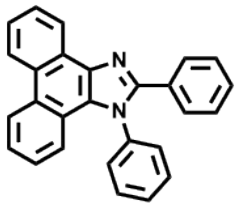

1

Compound 1: In a 100 ml round-bottom flask, benzaldehyde (200 mg, 1.8 mmol), phenanthrene-9,10-dione (470 mg, 2.2 mmol), aniline (701 mg, 7.5 mmol), NH_4OAc (581 mg, 7.5 mmol), and glacial acetic acid (25 ml) were taken and refluxed for 12 hours at 110°C. After the completion of the reaction, the mixture was cooled, poured into methanol, filtered, and dried to obtain **1** as the product (92 %). ^{1}H NMR (400 MHz, $CDCl_3$) δ 8.87 (d, *J* = 8.0 Hz, 1H), 8.76 (d, *J* = 8.4 Hz, 1H), 8.70 (d, *J* = 8.3 Hz, 1H), 7.74 (t, *J* = 7.5 Hz, 1H), 7.68 – 7.54 (m, 6H), 7.51– 7.48 (m, 3H), 7.31 – 7.23 (m, 4H), 7.17 (d, *J* = 8.3 Hz, 1H). ^{13}C NMR (100 MHz, $CDCl_3$) δ 151.01, 138.71, 137.38, 130.50, 130.13, 129.88, 129.48, 129.14, 128.86, 128.28. 128.23, 128.12, 127.32, 127.22, 126.33, 125.63, 124.90, 124.12, 123.14, 123.05, 122.76, 120.88. HRMS (ESI) (m/z): 371.1523 $[M+H]^+$; Calculated for $C_{27}H_{18}N_2$ + H: 371.1542 .

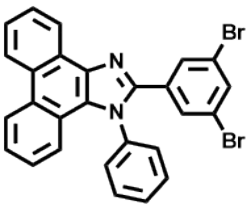

2

Compound 2: In a 100 ml round-bottom flask, 3,5-dibromobenzaldehyde (1000 mg, 3.7 mmol), phenanthrene-9,10-dione (948 mg, 4.5 mmol), aniline (1767 mg, 18.9 mmol), NH_4OAc (1170 mg, 15.2 mmol) and glacial acetic acid (25 ml) were taken and refluxed for 12 hours at 110°C. After the completion of the reaction, the mixture was cooled, poured into methanol, filtered, and dried. The residue was purified by column chromatography in petroleum ether/ethyl acetate on silica gel to get compound **2,** yielding 87 %. ^{1}H NMR (400 MHz, $CDCl_3$) δ 8.83 (d, *J* = 9.1 Hz, 1H), 8.75 (d, *J* = 8.3 Hz, 1H), 8.69 (d, *J* = 8.3 Hz, 1H), 7.77 – 7.62 (m, 7H), 7.59 (t, *J* = 1.7 Hz, 1H), 7.54 – 7.49 (m, 3H), 7.26 – 7.27 (m, 1H), 7.19 (dd, *J* = 8.4, 1.2 Hz, 1H). ^{13}C NMR (100 MHz, $CDCl_3$) δ 147.46, 138.14, 137.48, 134.10, 133.72, 130.75, 130.53, 130.37, 129.58, 128.87, 128.55, 128.40, 127.49, 127.00, 126.45, 125.97, 125.37, 124.19, 123.19, 122.79, 122.71, 122.68, 120.95. HRMS (ESI) (m/z): 526.9723 $[M+H]^+$; Calculated for $C_{27}H_{16}Br_2N_2$ + H: 526.9680.

The general procedure for the Suzuki cross-coupling reaction

Compound **2**, arylboronic acid, and 2M K_2CO_3 were added to toluene: ethanol (3:1, 15 mL) in a 100 mL two-neck round-bottom flask. The reaction was purged with nitrogen for 20 min, then $Pd(PPh_3)_4$ (0.05 eqv) was added. The reaction mixture was allowed to stir at 105 °C for 12 h under

a nitrogen atmosphere. After the completion of the reaction, the reaction mixture was poured over water, and the organic layer was extracted with dichloromethane. The organic layer was dried over anhydrous Na_2SO_4. The solvent was removed under reduced pressure, and the residue was purified by column chromatography on silica gel.

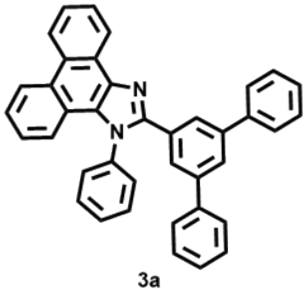

3a

Compound 3a: As per general procedure, compound **2** (150 mg, 0.28 mmol) and phenylboronic acid (138 mg, 1.1 mmol) were allowed to react to give product **3a**, and column chromatography was performed (petroleum ether/ethyl acetate) to obtain the compound with a yield of 84 %. ^{1}H NMR (400 MHz, $CDCl_3$) δ 8.92 (d, *J* = 8.0 Hz, 1H), 8.77 (d, *J* = 8.4 Hz, 1H), 8.70 (d, *J* = 8.3 Hz, 1H), 7.81 (d, *J* = 1.7 Hz, 2H), 7.78 – 7.72 (m, 2H), 7.72 – 7.64 (m, 4H), 7.64 – 7.58 (m, 2H), 7.53 – 7.45 (m, 5H), 7.45 – 7.39 (m, 4H), 7.38 – 7.32 (m, 2H), 7.30 – 7.22 (m, 2H). ^{13}C NMR (100 MHz, $CDCl_3$) δ 150.58, 141.67, 140.57, 139.07, 137.49, 131.27, 130.41, 129.85, 129.36, 128.79, 128.36, 128.26, 127.63, 127.39, 127.26, 127.21, 126.40, 126.35, 125.72, 125.01, 124.19, 123.12, 123.05, 122.83, 120.96. HRMS (ESI) (m/z): 523.2140 $[M+H]^+$; Calculated for $C_{39}H_{26}N_2$ + H: 523.2096.

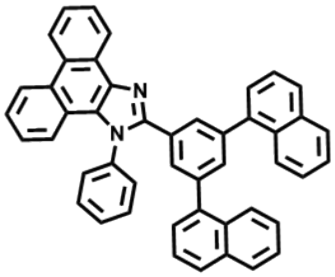

3b

Compound 3b: Compound **2** (200 mg, 0.37 mmol) and 2-naphthylboronic acid (260 mg, 1.5 mmol) were allowed to react as per the general procedure. The product was isolated by column chromatography on silica gel (petroleum ether/ethyl acetate) with a yield of 80 %. ^{1}H NMR (400 MHz, $CDCl_3$) δ 8.96 (d, *J* = 8.0 Hz, 1H), 8.80 (d, *J* = 8.5 Hz, 1H), 8.74 (d, *J* = 8.3 Hz, 1H), 8.01 – 7.98 (m, 3H), 7.94 – 7.88 (m, 8H), 7.85 – 7.75 (m, 4H), 7.70 – 7.66 (m, 5H), 7.56 – 7.49 (m, 5H), 7.33 – 7.28 (m, 2H). ^{13}C NMR (100 MHz, $CDCl_3$) δ 150.48, 141.67, 139.21, 137.87, 137.53, 133.64, 132.78, 131.41, 130.54, 129.98, 129.48, 129.42, 128.50, 128.36, 128.32, 128.24, 127.70, 127.49, 127.43, 127.23, 126.80, 126.41, 126.36, 126.15, 126.09, 125.74, 125.48, 125.04, 124.21, 123.19, 123.05, 122.83, 120.98. HRMS (ESI) (m/z): 623.2424 $[M+H]^+$; Calculated for $C_{47}H_{30}N_2$ + H: 623.2409.

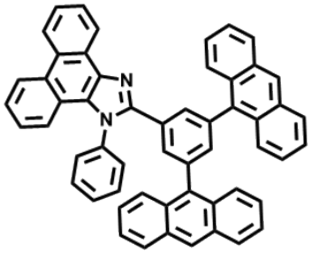

3c

Compound 3c: In a round-bottom flask, compound **2** (100 mg, 0.19 mmol) and 9-anthraceneboronic acid (168 mg, 0.7 mmol) were taken, and the reaction was performed as per the general procedure. The column chromatography was done in petroleum ether/ethyl acetate to obtain compound **3c** with a yield of 84 %. ^{1}H NMR (400 MHz, $CDCl_3$) δ 8.82 (d, *J* = 8.1 Hz, 1H), 8.73 (d, *J* = 8.3 Hz, 1H), 8.67 (d, *J* = 8.3 Hz, 1H), 8.46 (s, 2H), 8.01 (d, *J* = 8.1 Hz, 4H), 7.84 (d, *J* = 1.6 Hz, 2H), 7.73 – 7.67 (m, 5H), 7.64 –7.59 (m, 1H), 7.56 – 7.51 (m, 5H), 7.49 – 7.43 (m, 7H), 7.42 – 7.39 (m, 2H), 7.26 – 7.20 (m, 3H). ^{13}C NMR (100 MHz, $CDCl_3$) δ 151.04, 138.96, 138.59, 137.34, 135.64, 137.99, 137.90, 131.29, 131.17, 130.16, 129.84, 129.31, 129.16, 128.41, 128.28, 128.13, 127.33, 127.22, 126.97, 126.67, 126.32, 125.66, 125.12, 124.99, 124.11, 123.12, 122.97, 122.77, 120.86. HRMS (ESI) (m/z): 723.2756 $[M+H]^+$; Calculated for $C_{55}H_{34}N_2$ + H: 723.2722.

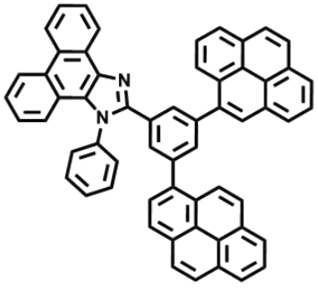

3d

Compound 3d: Compound **2** (150 mg, 0.28 mmol) and pyrene-1-boronic acid (279.5 mg, 1.1 mmol) were allowed to react according to the general procedure. Column chromatography was performed using petroleum ether/ethyl acetate. The product **3d** was obtained with a yield of 69 %. ^{1}H NMR (400 MHz, $CDCl_3$) δ 8.89 (d, *J* = 7.2 Hz, 1H), 8.76 (d, *J* = 8.3 Hz, 1H), 8.69 (d, *J* = 8.3 Hz, 1H), 8.20 – 8.15 (m, 7H), 8.07 – 7.97 (m, 9H), 7.92 (d, *J* = 8.0 Hz, 2H), 7.85 (t, *J* = 1.6 Hz, 1H), 7.75 – 7.62 (m, 7H), 7.56 – 7.48 (m, 2H), 7.29 – 7.20 (m, 3H). ^{13}C NMR (100 MHz, $CDCl_3$) δ 150.78, 141.35, 138.81, 137.50, 136.70, 133.41, 131.45, 130.95, 130.92, 130.81, 130.60, 130.43, 129.96, 129.39, 128.46, 128.33, 127.88, 127.83, 127.60, 127.41, 127.21, 126.35, 126.08, 125.72, 125.25, 125.01, 124.96, 124.93, 124.85, 124.69, 124.16, 123.15, 123.04, 122.83, 120.92 HRMS (ESI) (m/z): 771.2764 $[M+H]^+$; Calculated for $C_{59}H_{34}N_2$ + H: 771.2722.

3. ^{1}H, ^{13}C NMR, and HRMS spectra of the synthesized compounds

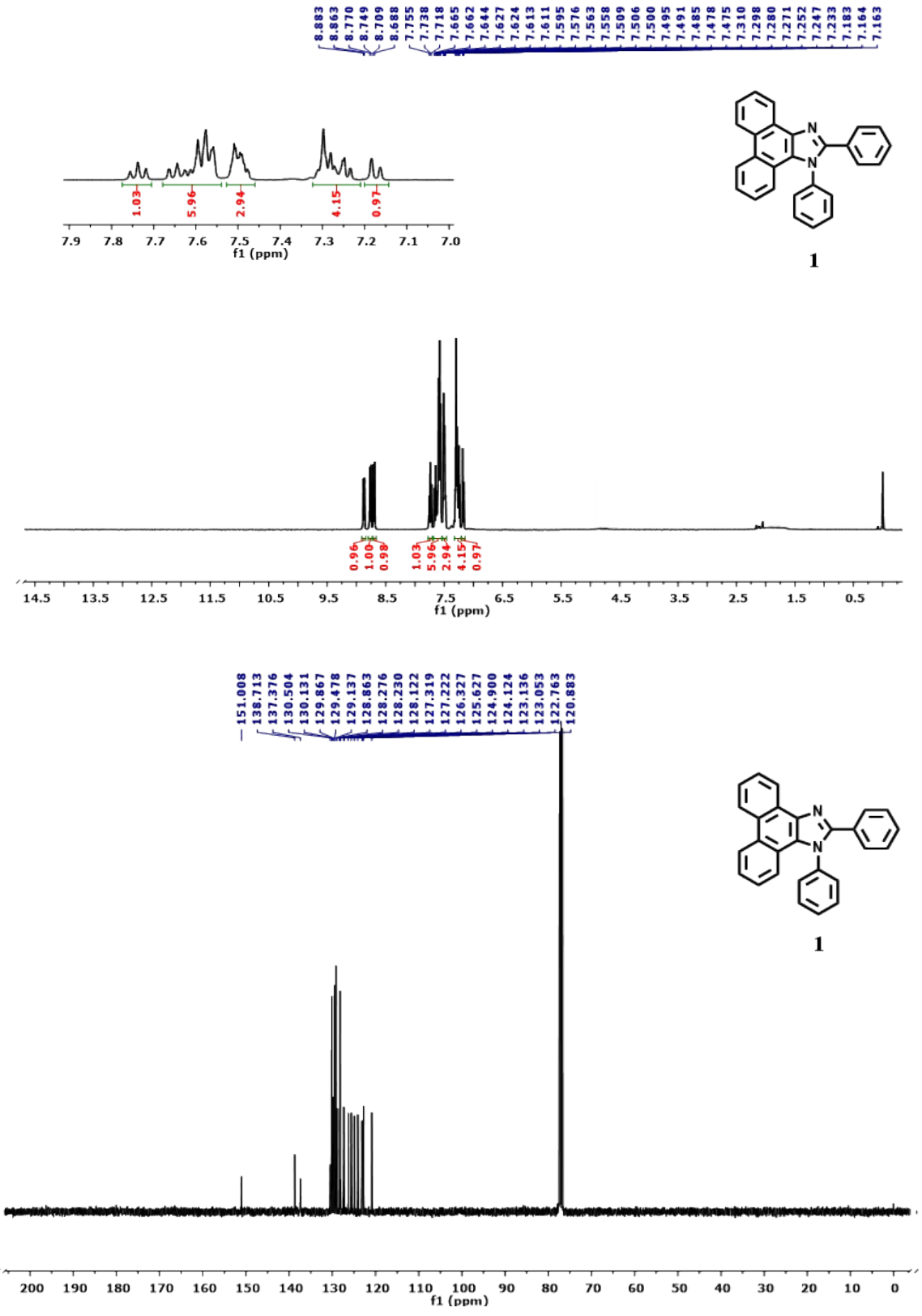

Figure S1. ^{1}H and ^{13}C NMR spectra of compound **1**

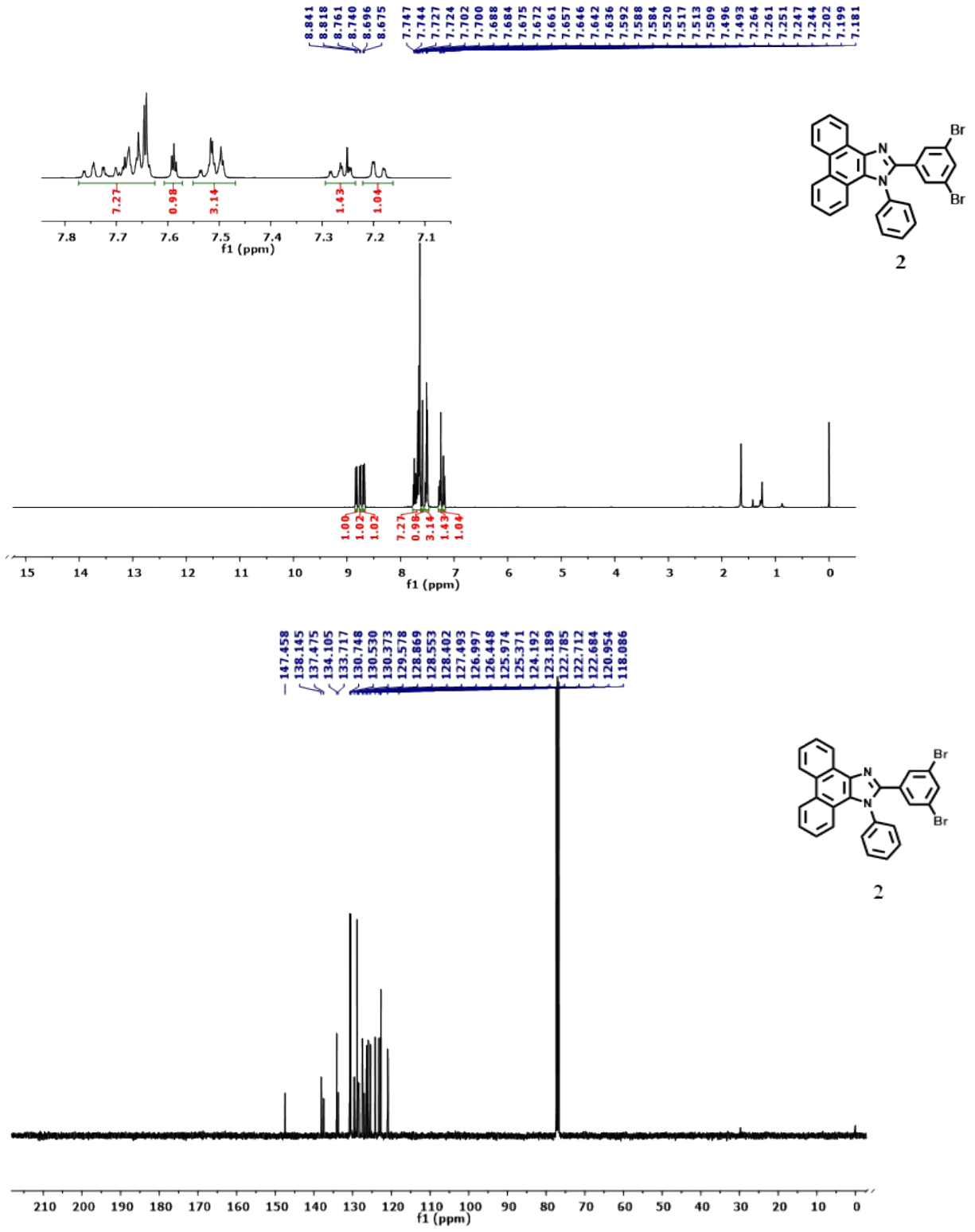

Figure S2. ^{1}H and ^{13}C NMR spectra of compound **2**

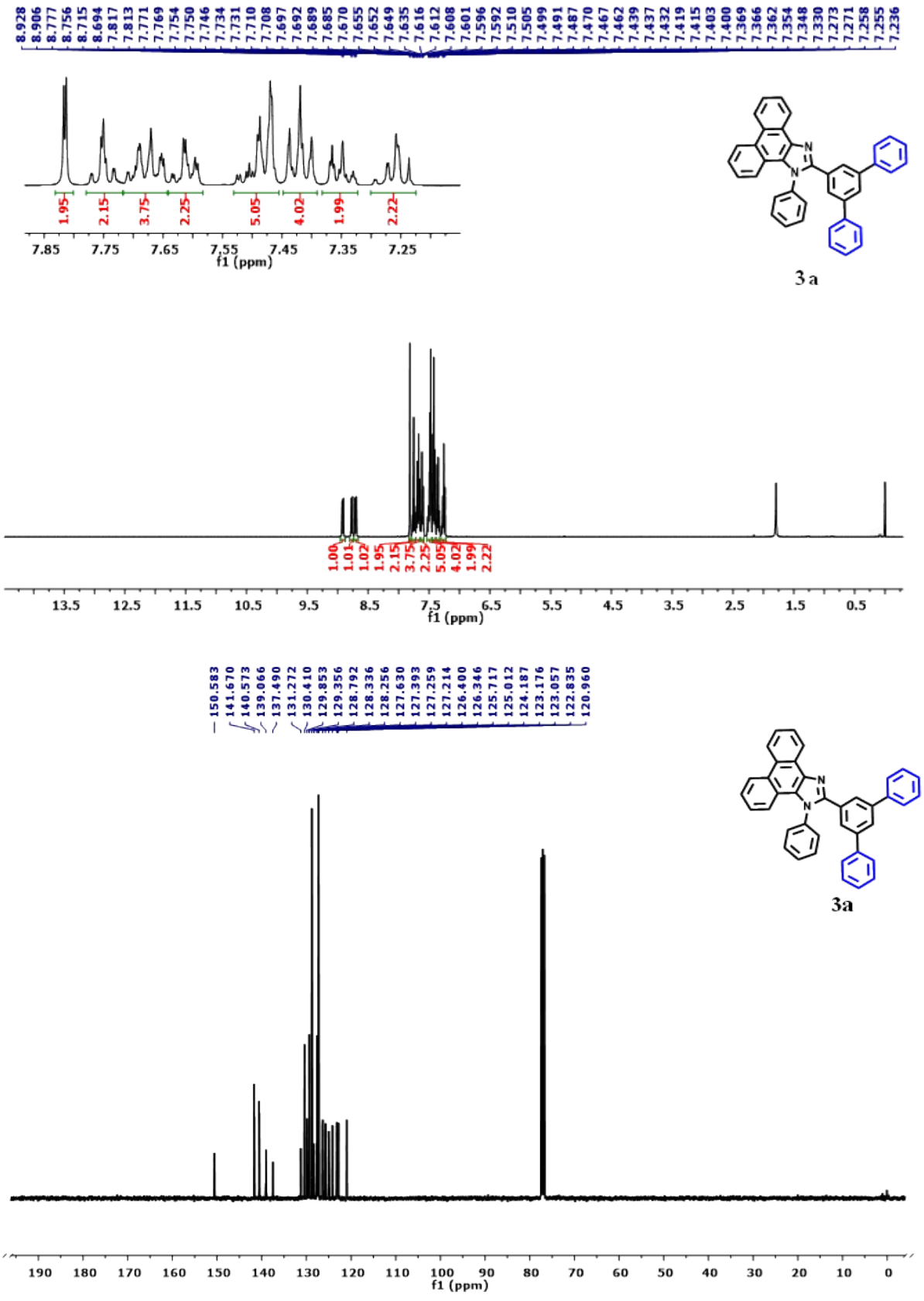

Figure S3. ^{1}H and ^{13}C NMR spectra of compound **3a**

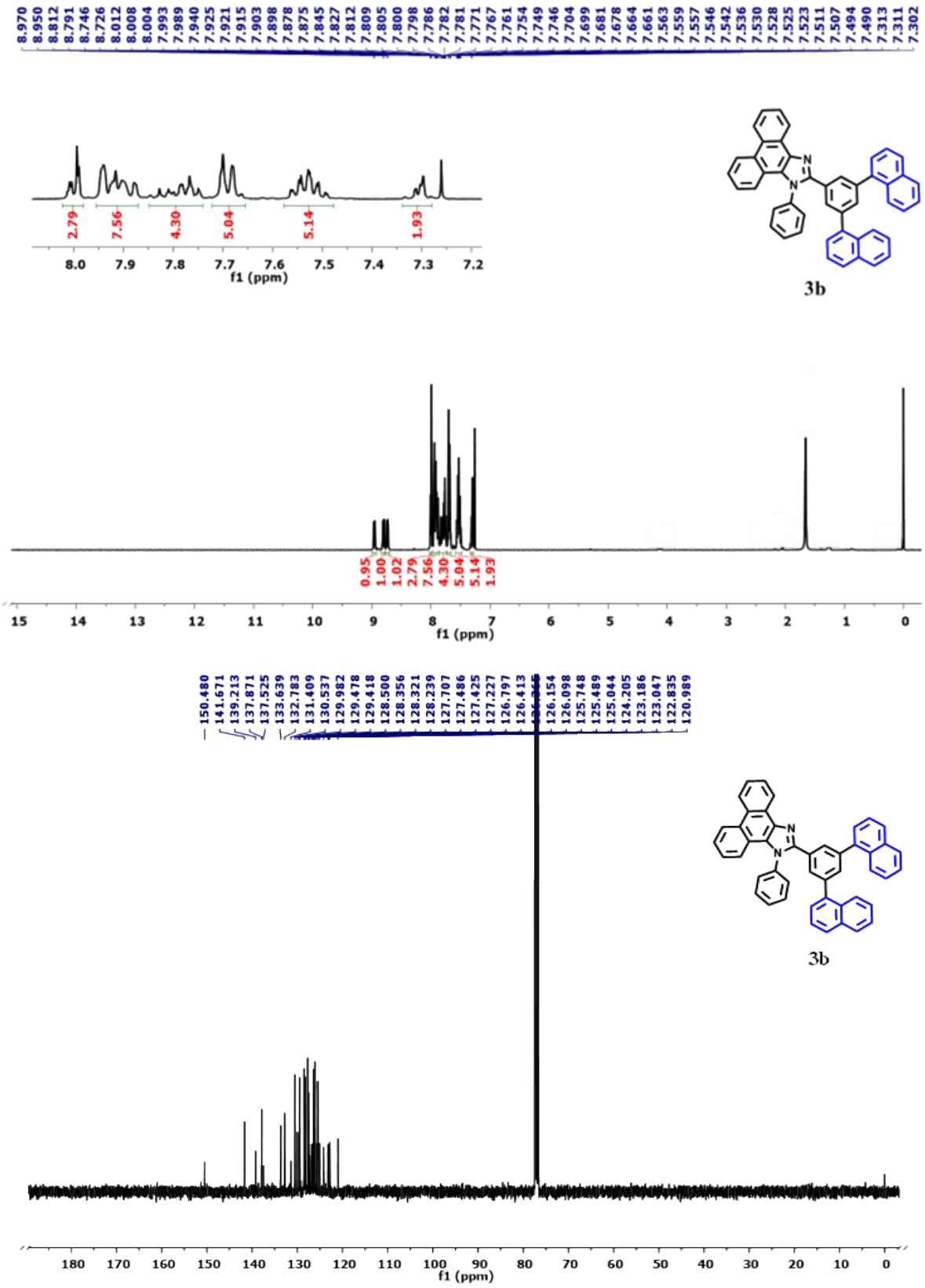

Figure S4. ^{1}H and ^{13}C NMR spectra of compound **3b**

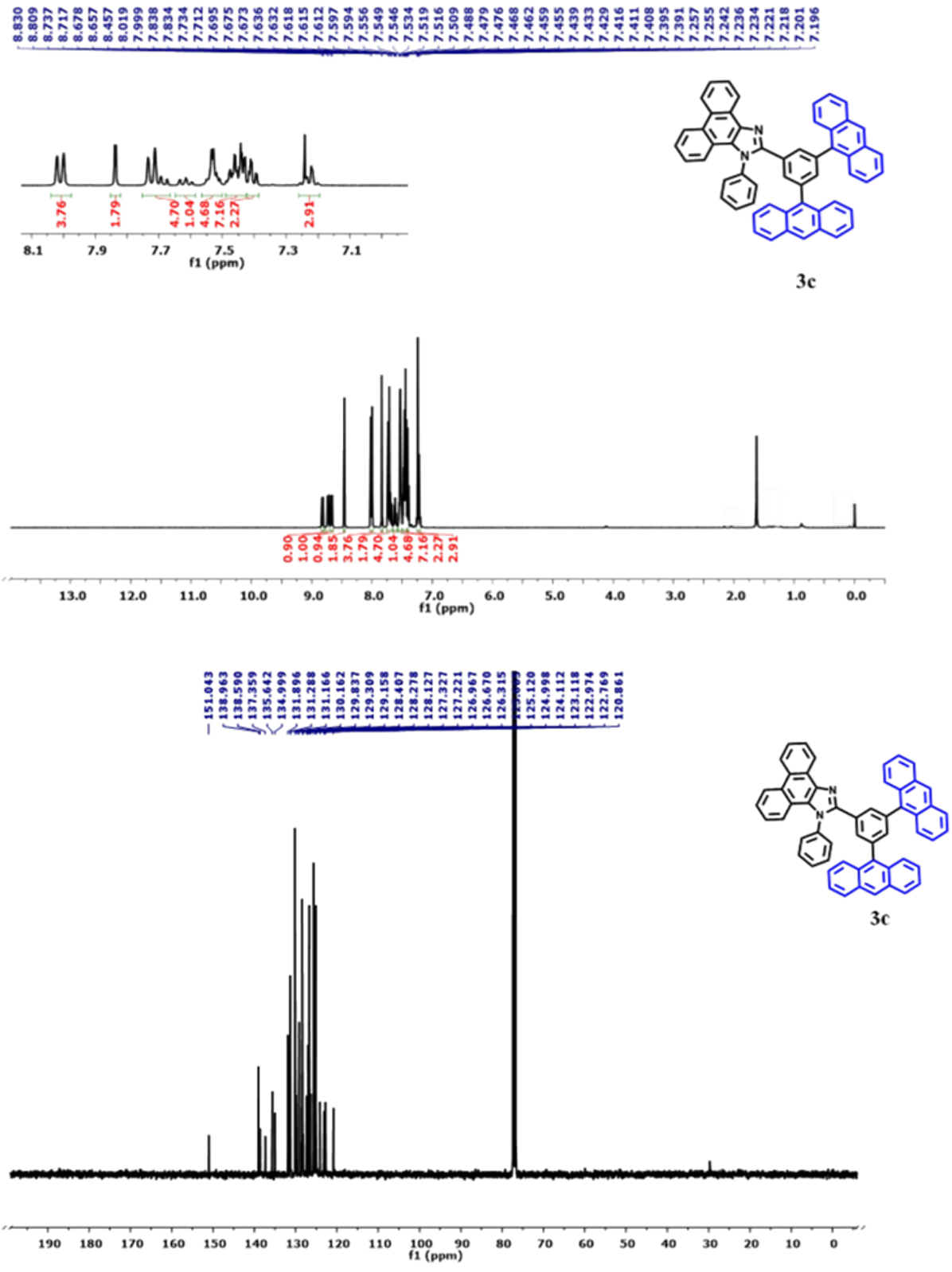

Figure S5. ^{1}H and ^{13}C NMR spectra of compound **3c**

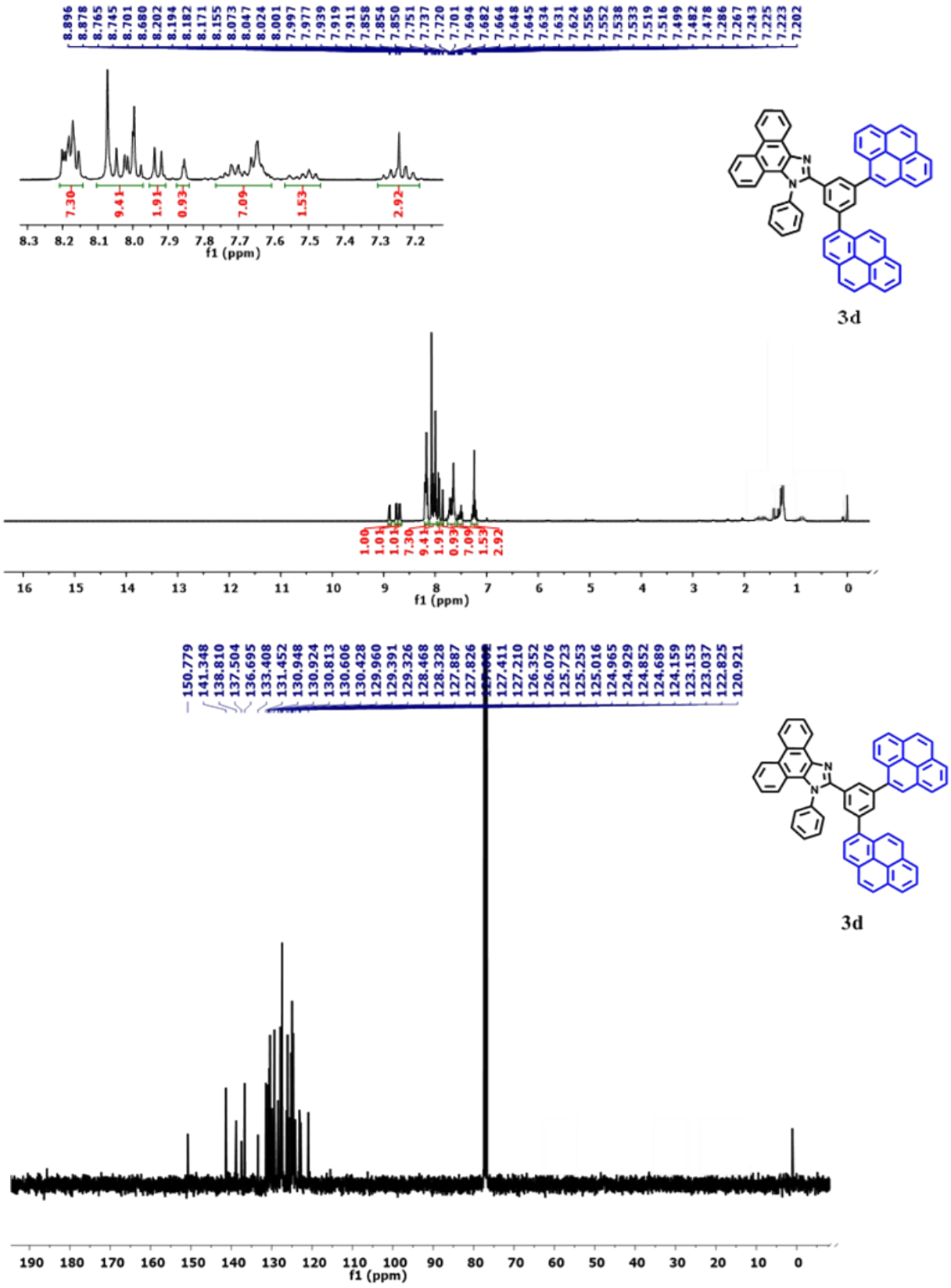

Figure S6. ^{1}H and ^{13}C NMR spectra of compound **3d**

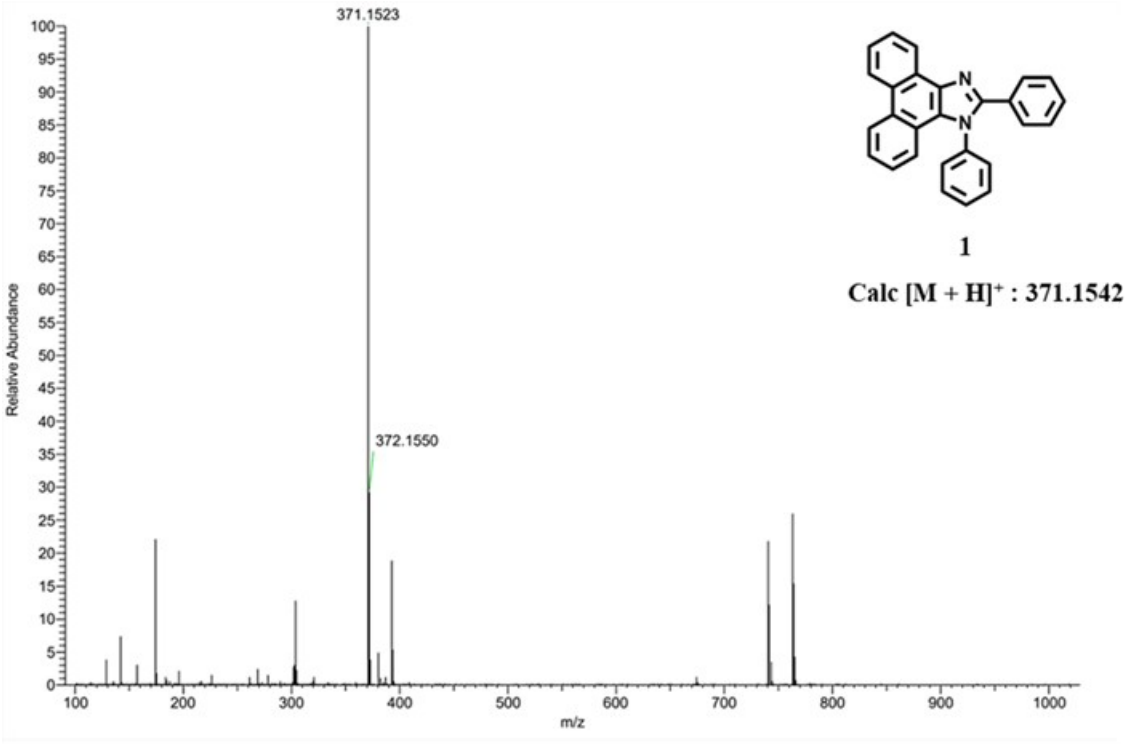

Figure S7. HRMS spectrum of compound **1**

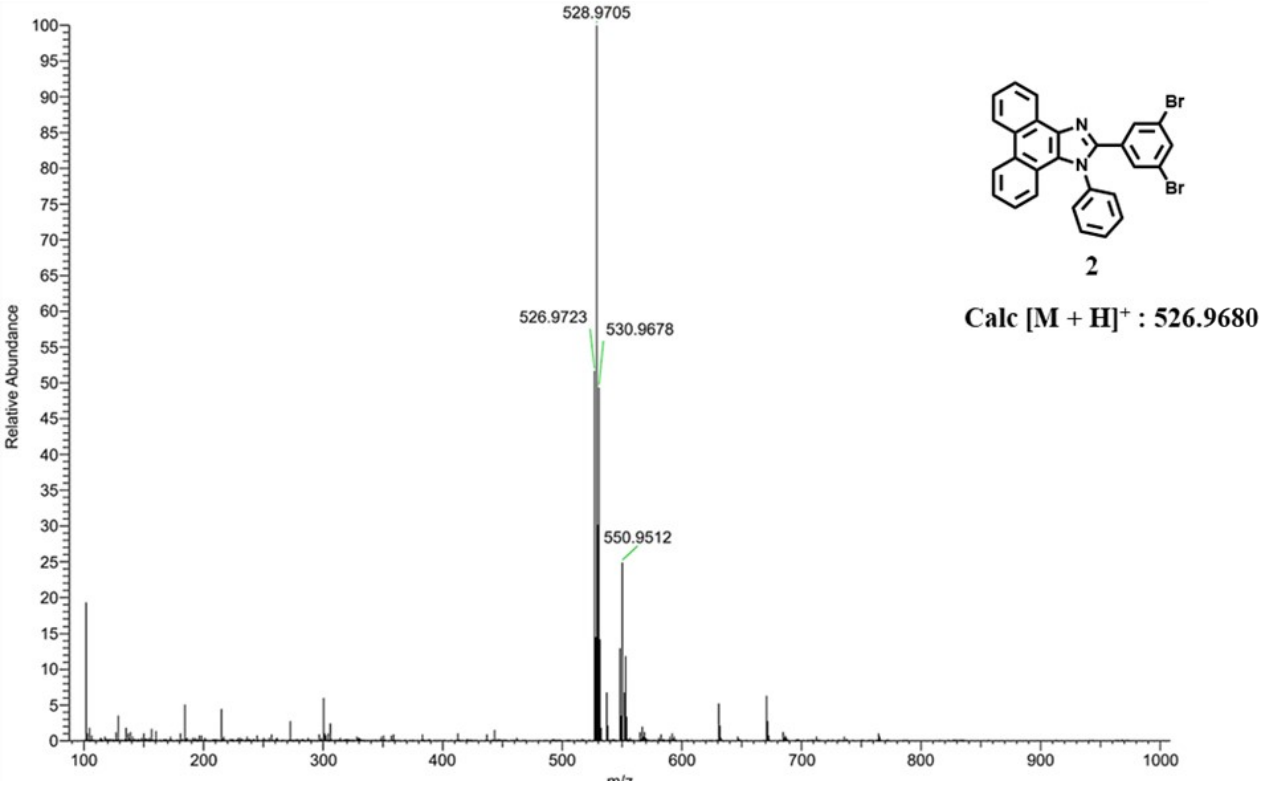

Figure S8. HRMS spectrum of compound **2**

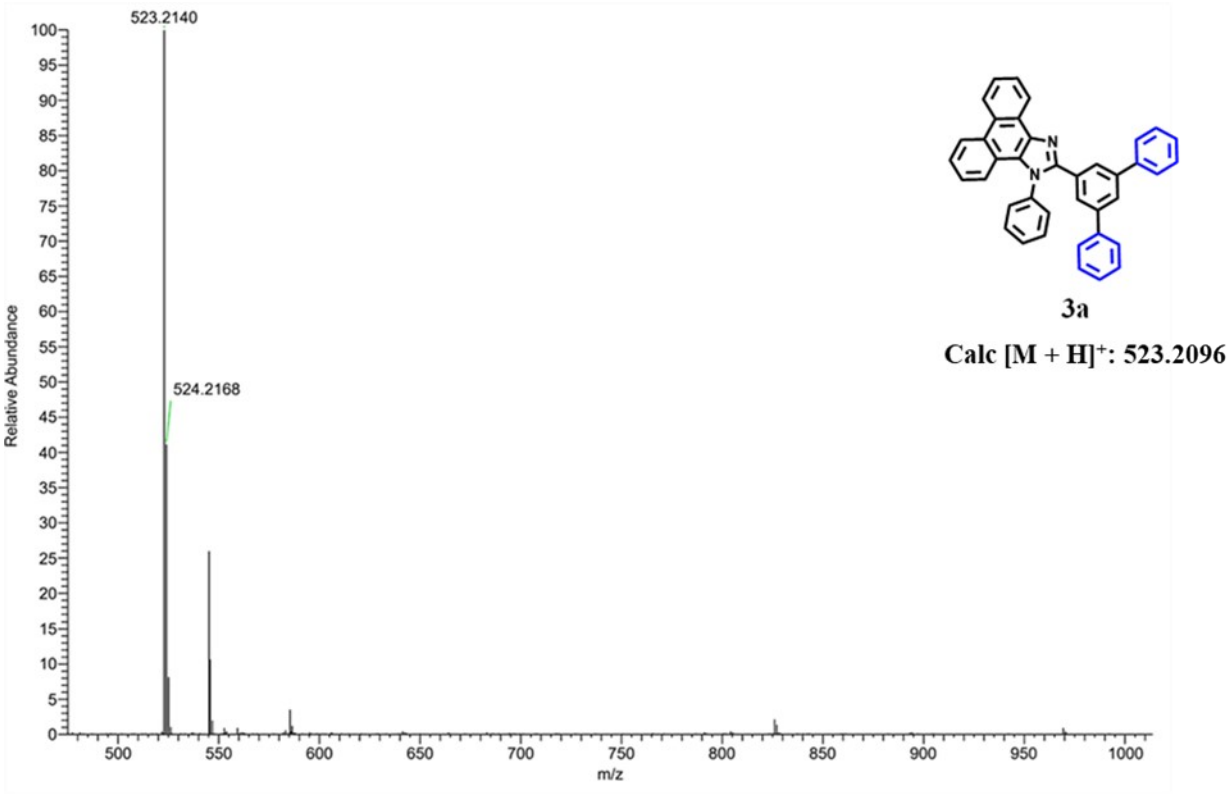

Figure S9. HRMS spectrum of compound **3a**

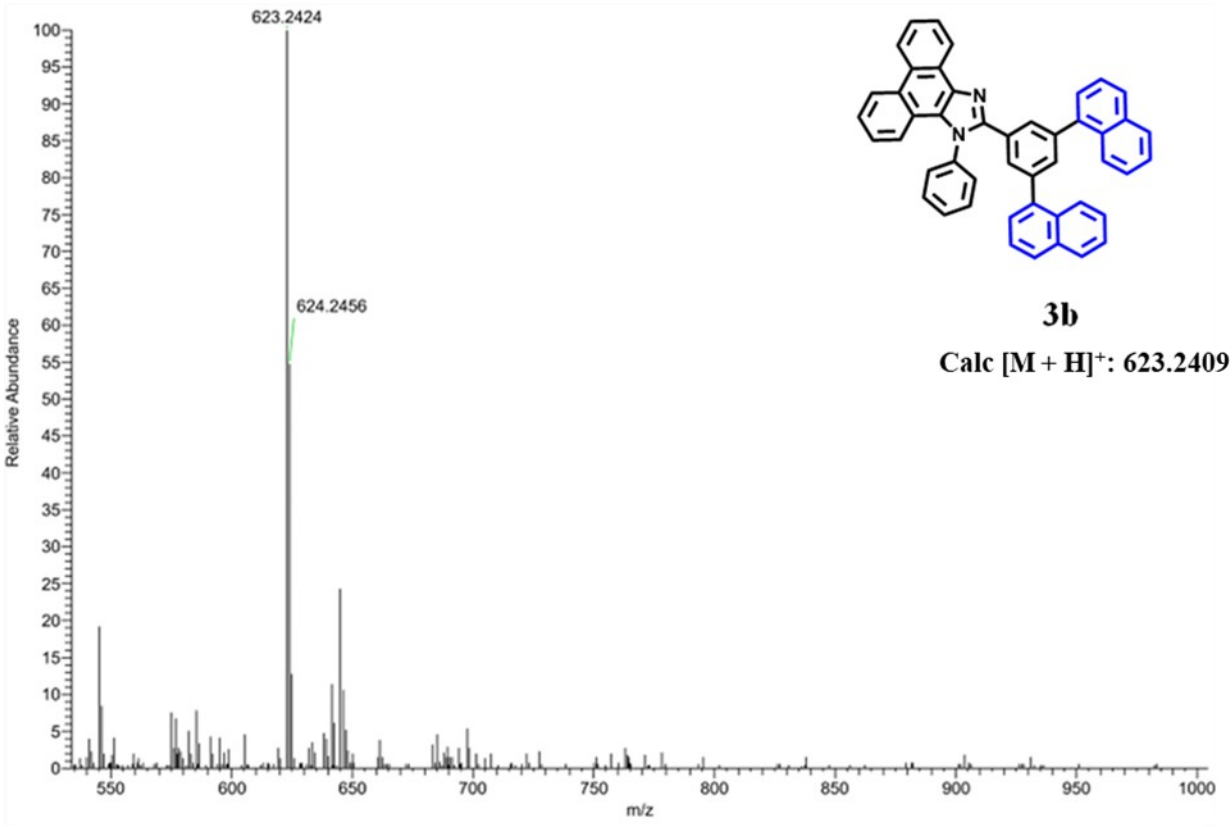

Figure S10. HRMS spectrum of compound **3b**

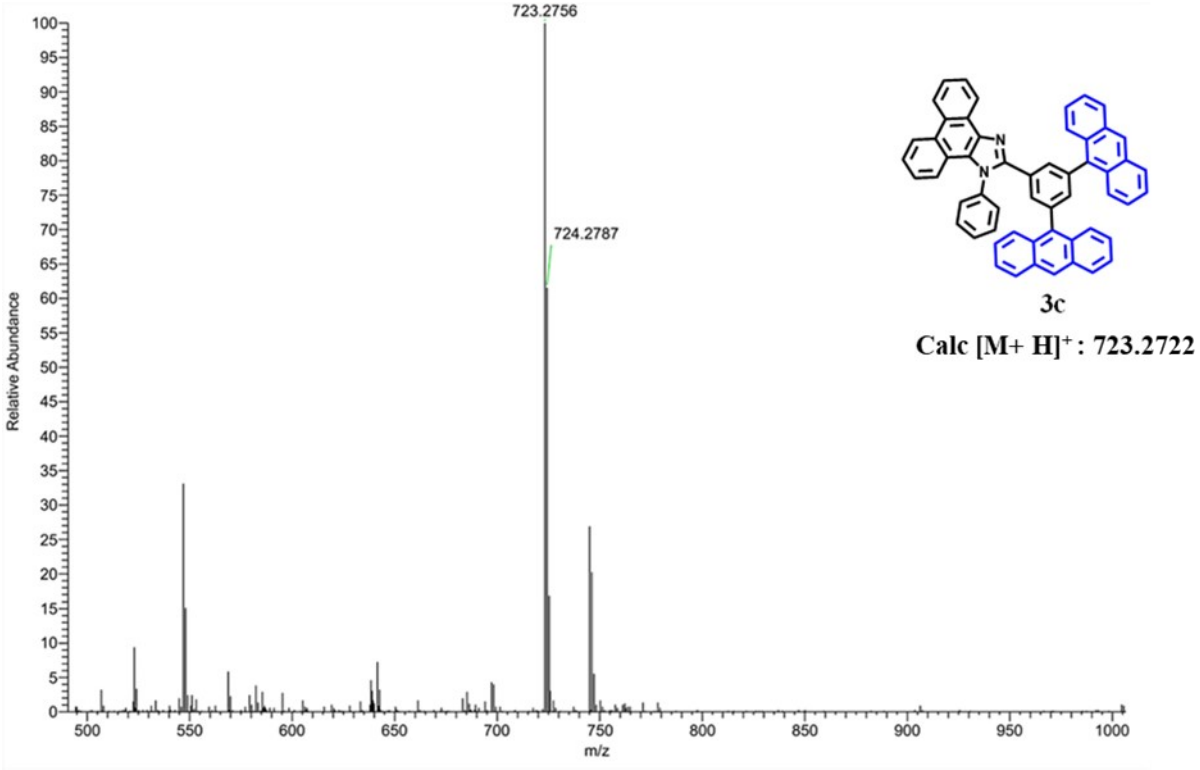

Figure S11. HRMS spectrum of compound **3c**

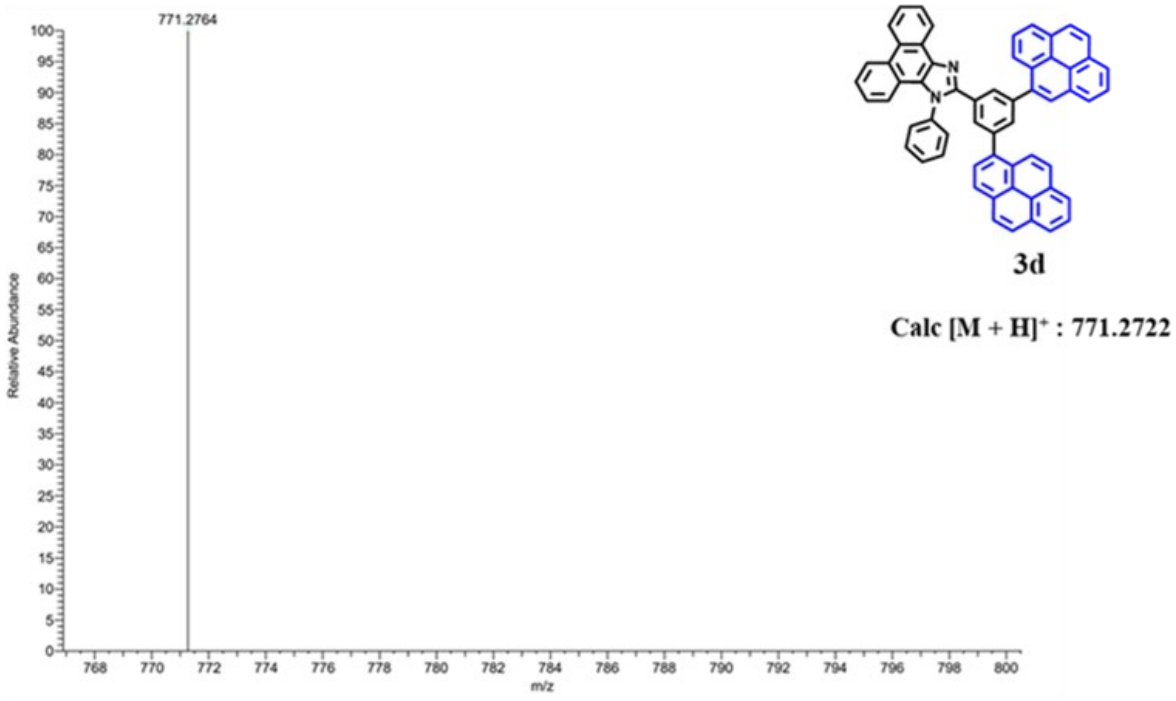

Figure S12. HRMS spectrum of compound **3d**

4. Thermal Properties

Table S1. Thermal properties of compounds **1, 3a-d**

Compounds	T_d (°C)
1	292.64
3a	396.60
3b	281.85
3c	492.95
3d	536.74

[a] T_d is the decomposition temperature

5. Electrochemical Analysis

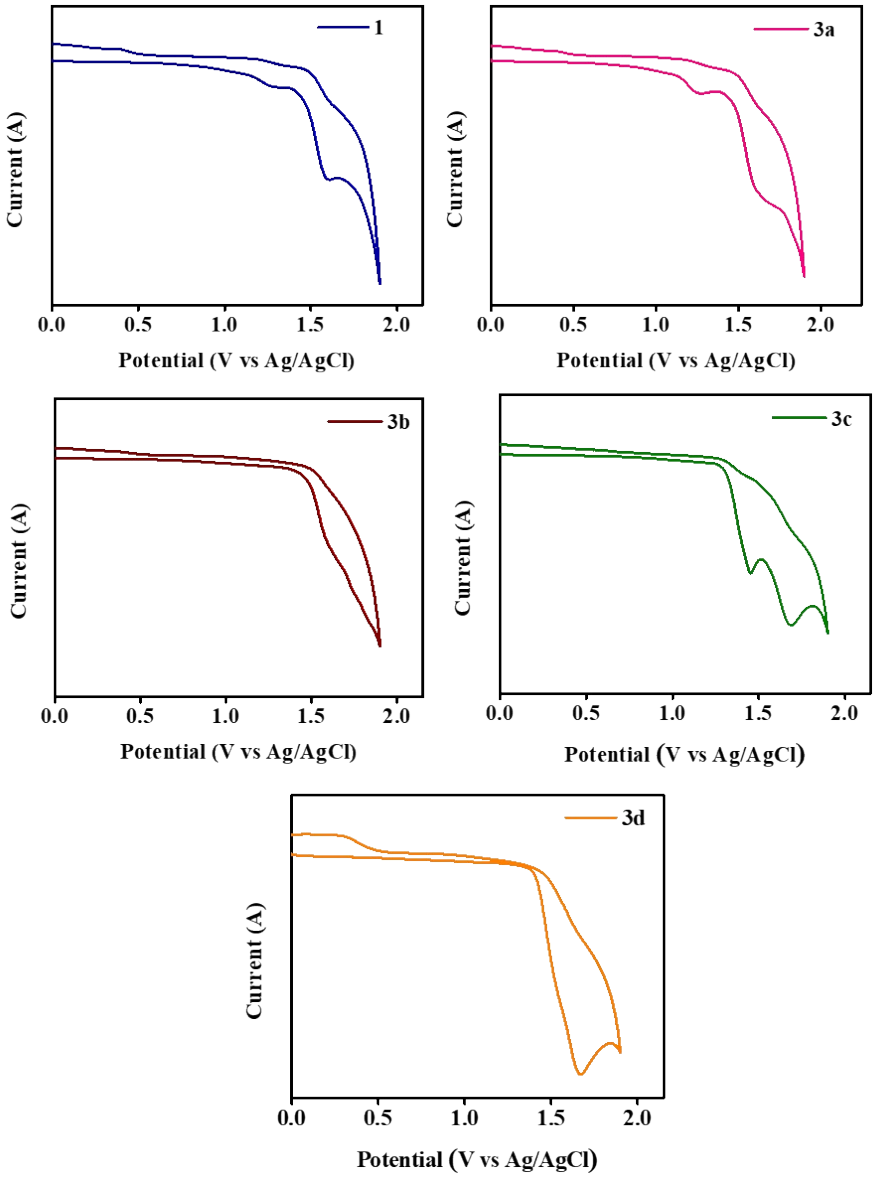

Figure S13. Cyclic Voltammogram of compounds **1**, **3a-d**

Single-crystal study of compound 3b

CCDC	**2480791**	
Emperical formula	$C_{47}H_{30}N_2$	
Formula weight	622.73	
Temperature	100.00(10) K	
Wavelength	1.54184 Å	
Crystal system	triclinic	
Space group	*P*-1	
Unit cell dimensions	a =11.3454(2) Å	α = 69.537(2)°
	b =12.08420(10) Å	β = 80.214(2)°
	c =12.4389(3) Å	γ =88.2640(10)°
Volume	1573.73(5) Å^3	
Z	2	
Density (calculated)	1.314 g/cm^3	
Absorption coefficient	0.583 mm^{-1}	
F(000)	652	
Crystal size	0.53 × 0.27 × 0.08 mm^3	
Theta range for data collection	3.849 to 80.171 °	
Reflections collected	62661	
Independent reflections	6791 [R_{int} = 0.0378]	
Completeness to theta = 80.171°	100.00 %	
Max. and min. transmission	1.000 and 0.417	
Refinement method	Full-matrix least-squares on F^2	
Goodness-of-fit on F^2	1.061	
Final R indices [I>2sigma(I)]	R_1 =0.0414, wR_2 = 0.1077	
R indices (all data)	R_1 = 0.0426, wR_2 = 0.1087	
Extinction coefficient	n/a	
Largest diff. peak and hole	0.320 and -0.229 e. Å^{-3}	

Single-crystal study of compound 3c

CCDC	**2480792**
Emperical formula	$C_{55}H_{34}N_2$
Formula weight	722.84
Temperature	99.99(10) K
Wavelength	1.54184 Å
Crystal system	monoclinic
Space group	$P2_1/c$
Unit cell dimensions	a =21.56900(10) Å $\alpha = 90^\circ$
	b =9.18850(10) Å $\beta = 93.6180(10)^\circ$
	c =18.70500(10) Å $\gamma = 90^\circ$
Volume	3699.69(5) Å
Z	4
Density (calculated)	1.298 Mg/m^3
Absorption coefficient	0.574 mm^{-1}
F(000)	1512
Crystal size	0.68 × 0.43 × 0.18 mm^3
Theta range for data collection	4.107 to 80.174°
Reflections collected	75340
Independent reflections	8026 [R_{int} = 0.0414]
Completeness to theta = 80.174°	100 %
Max. and min. transmission	1.000 and 0.350
Refinement method	Full-matrix least-squares on F^2
Goodness-of-fit on F^2	1.035
Final R indices [I>2sigma(I)]	R_1 =0.0366, wR_2 = 0.0931
R indices (all data)	R_1 =0.0380, wR_2 = 0.0942
Extinction coefficient	n/a
Largest diff. peak and hole	0.238 and -0.209 e. $Å^{-3}$

6. Thin film characterization studies

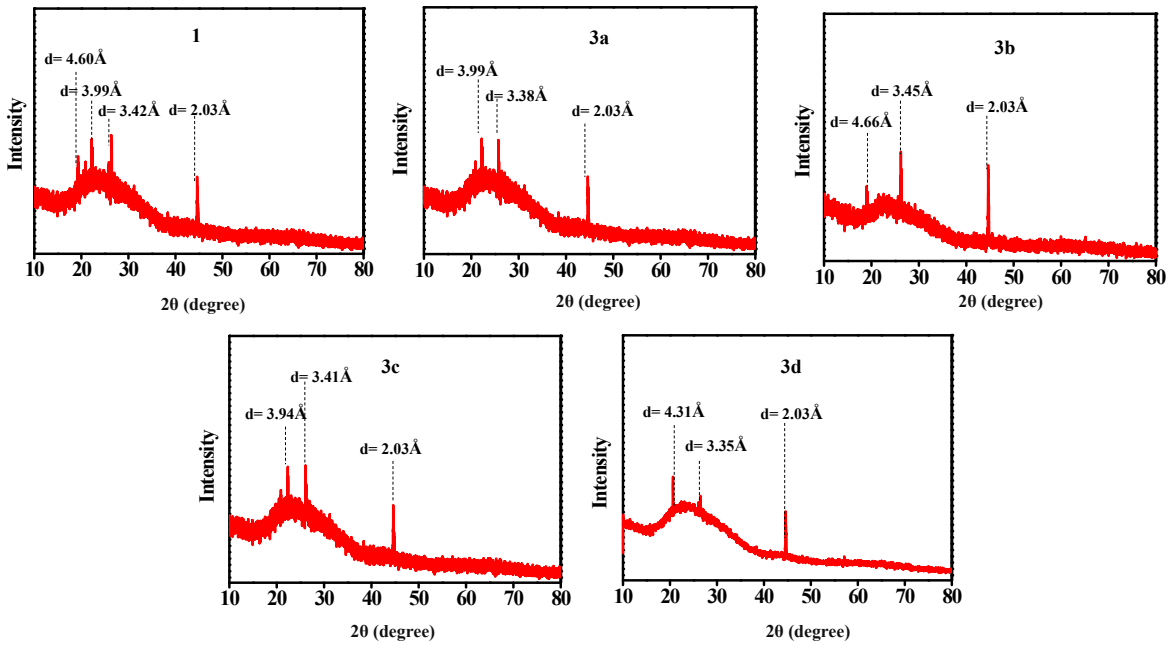

Figure S14. Thin-film GI-XRD of the compounds **1, 3a-d**

Table S2. GI-XRD diffraction data for compounds **1** and **3a–d**

Compounds	Peak Position (2θ)	d-spacing (Å)
1	19.24°, 22.22°, 26.30°	4.60, 3.99, 3.42
3a	22.22°, 26.30°	3.99, 3.38
3b	19.02°, 25.76°	4.66, 3.45
3c	22.32°, 26.08°	3.94, 3.41
3d	20.57°, 26.42°	4.31, 3.35
All	44.64°	2.03

7. Fabrication of the memory device

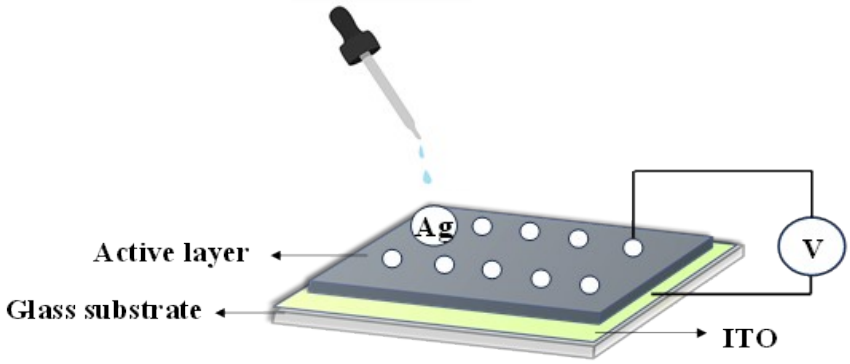

Figure S15. Schematic representation of the fabricated device

8. Memory Characteristics

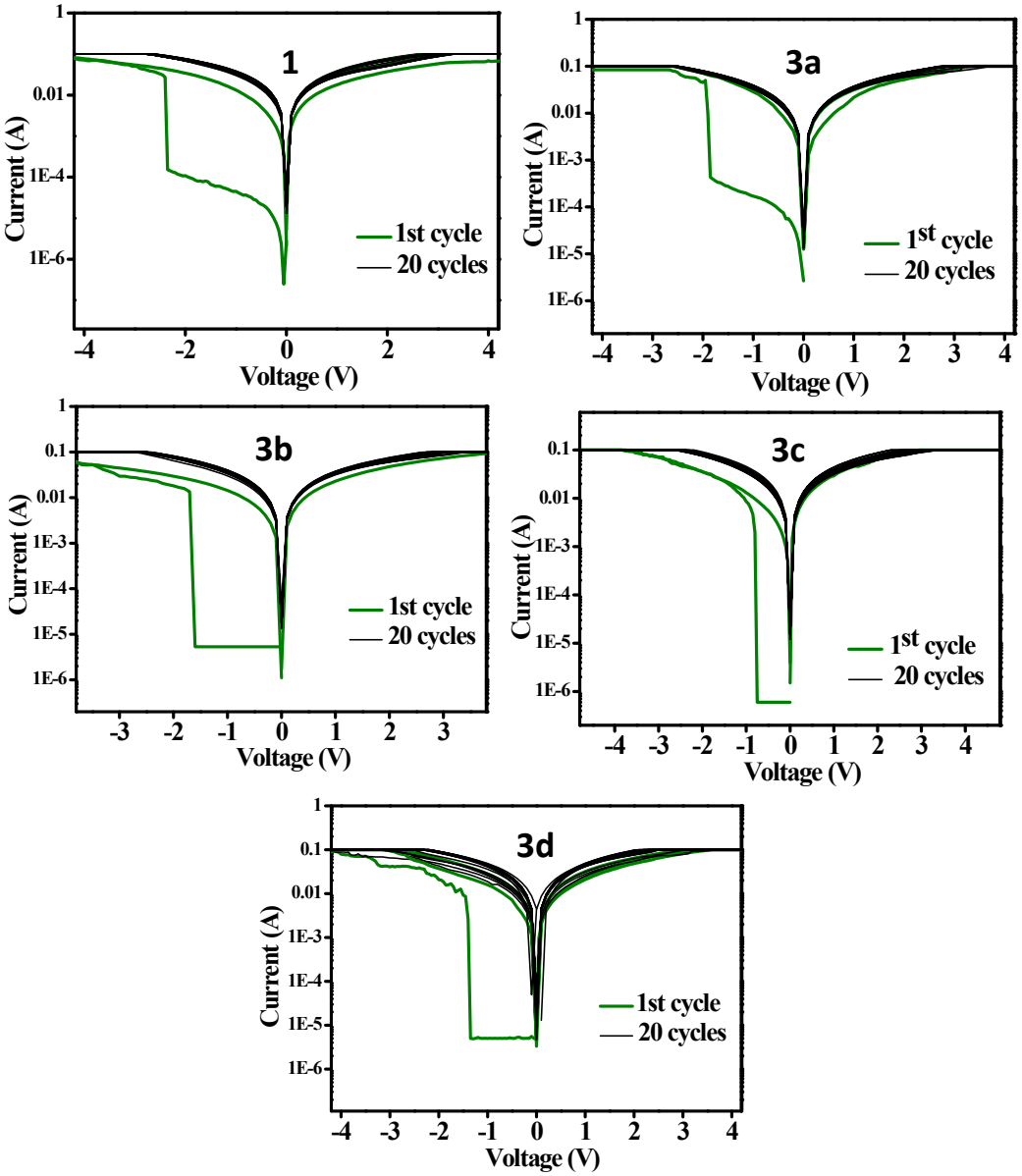

Figure S16. Cycle I-V characteristics over 20 consecutive sweeps of the devices ITO/ **1, 3a-d**/Ag

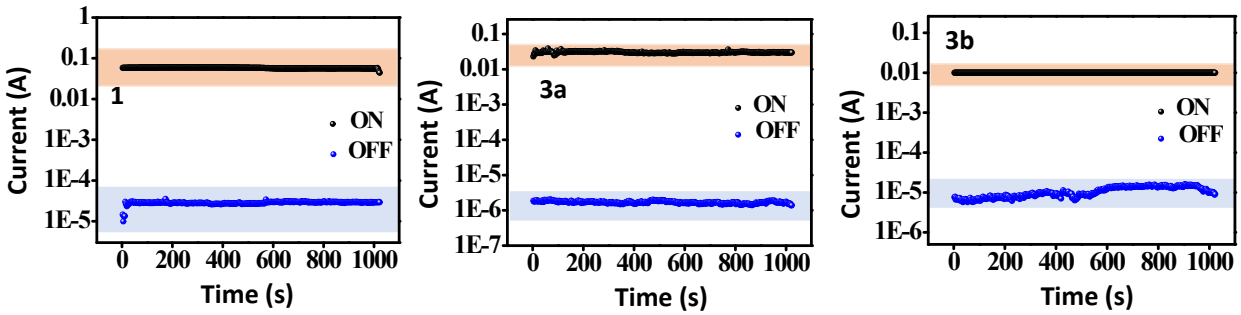

Figure S17. Retention time of the devices ITO/ **1, 3a-b**/Ag

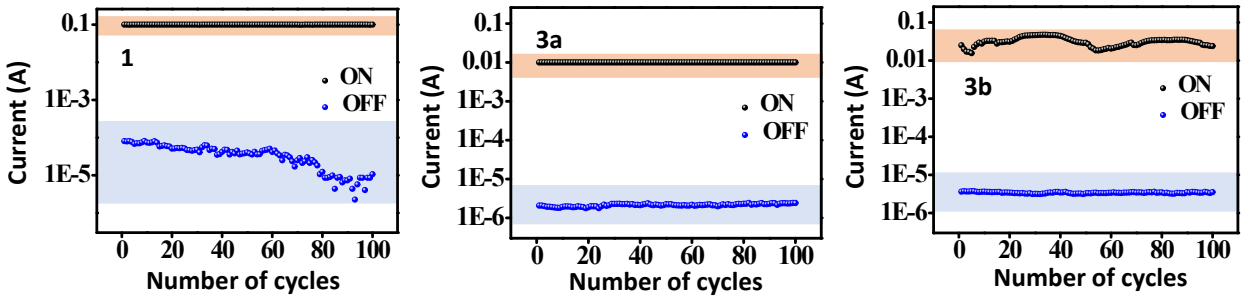

Figure S18. Endurance cycle of the device ITO/**1**, **3a-b**/Ag

9. Density functional theory (DFT) calculations

The computational analyses were conducted to gain deeper insights into the synthesized compounds' molecular packing and electronic properties. Geometry optimizations were performed using Density Functional Theory (DFT) at the B3LYP level with the 6-31D basis set, as implemented in the Gaussian software. Time-dependent self-consistent field (TD-SCF) calculations were also carried out to simulate UV–vis and fluorescence spectra, enabling comparison with experimental results and providing information on the electronic excited states.

Table S3. The predicted photophysical properties of the compounds **1, 3a-d**

Compounds	Absorption wavelength (nm)	Electronic transition	Emission wavelength (nm)	Electronic transition	Dipole moment (D)
1	314.4	$S_0 - S_1$	333.1	$S_0 - S_1$	3.976
3a	306.7	$S_0 - S_5$	383.6	$S_0 - S_1$	3.795
3b	301.9	$S_{-1} - S_2$	381.8	$S_0 - S_1$	2.363
3c	361.3	$S_{-2} - S_{-1}$	397.9	$S_0 - S_1$	1.984
3d	352.2	$S_{-2} - S_2$	392.2	$S_0 - S_1$	3.785

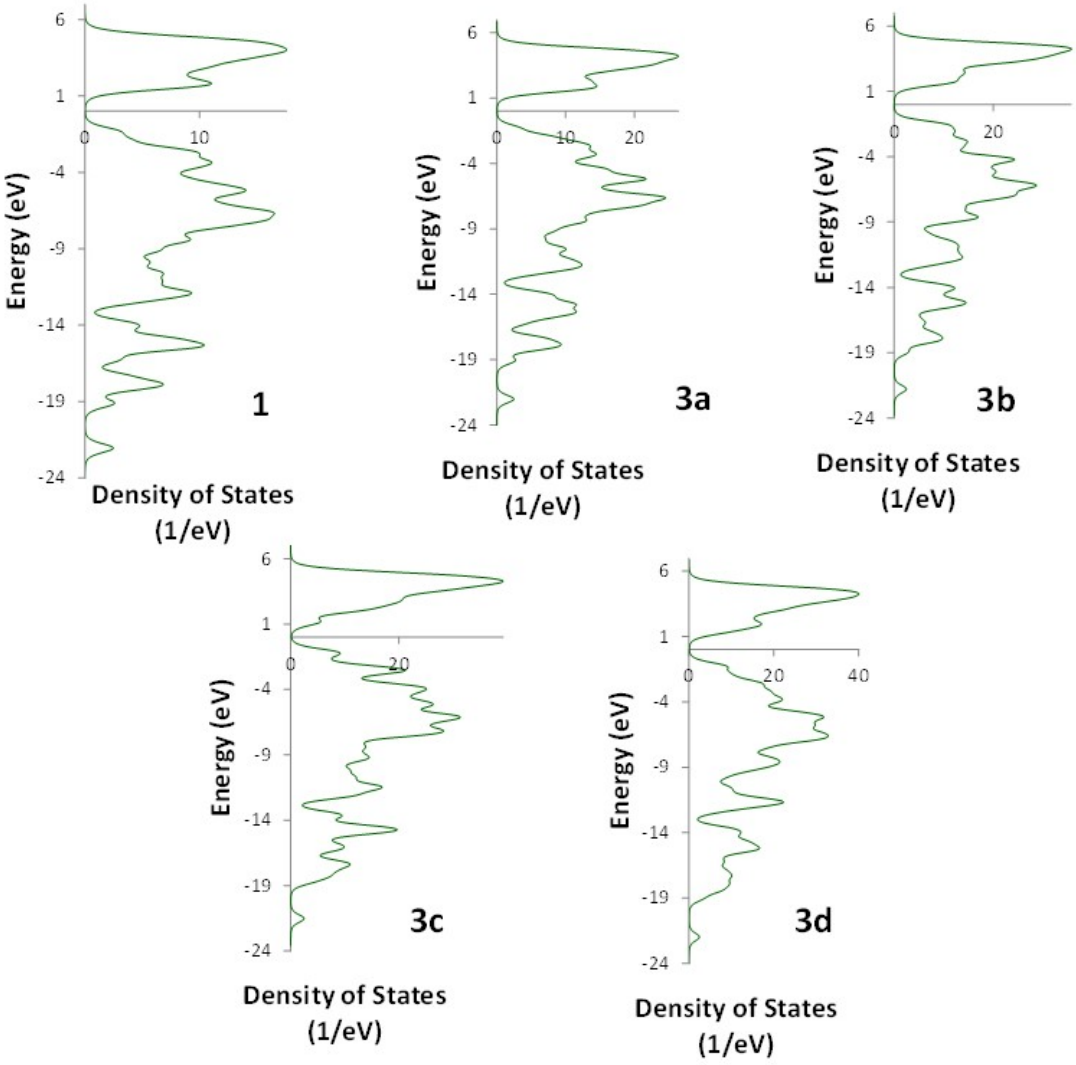

Figure S19. Graph of the density of state of compounds **1, 3a-d**

Table S4. DOS energy gap and E Fermi energy level of compounds **1, 3a-d**

Compounds	Molecular Formula	Free Energy (eV)	Density (mg/m³)	DOS Gap (eV)	E Fermi (eV)
1	$C_{27}N_2H_{18}$	-327.54	0.352	2.766	-3.453
3a	$C_{39}N_2H_{26}$	-465.82	0.312	2.711	-2.464
3b	$C_{47}N_2H_{30}$	-551.93	0.168	3.018	-3.224
3c	$C_{55}N_2H_{34}$	-638.97	0.254	2.112	-2.965
3d	$C_{59}N_2H_{34}$	-677.94	0.279	2.503	-3.841

Density of States (DOS) analysis was carried out using the PBE function to get an idea on the Fermi levels of the molecules.[1,2] It offered crucial insights into the number of electronic states available for particle movement,[3] while Fermi gap calculations helped to evaluate electron mobility.[4] The computed DOS values provided a deeper understanding of molecular Fermi levels, clarifying the distribution of electrons at specific energy levels. When the Fermi levels were closer, electronic transitions from the ground to the excited state occurred more easily. A lower DOS band gap indicated easier excitation and electron transport from lower energy to higher energy levels. The density of the state graphs of compounds **1, 3a-d** is given in **Figure S19,** and **Table S4** summarizes the DOS gap and E-Fermi energy levels of the synthesized compounds **1, 3a-d**. The DOS band gap value is the least for compound **3c**; hence, compound **3c** shows easy excitation or transport of particles from lower energy to higher energy levels.

8. Crystalline parameters and packing pattern

Additionally, VASP MedeA[5] reference software simulations were utilized to accurately predict the crystalline structure of the synthesized compounds, enabling a detailed examination of interatomic distances, where the solvent correction parameter was also encompassed. The findings revealed that reduced interatomic distances promoted favorable molecular packing, enhancing intermolecular interactions and facilitating efficient charge transfer.

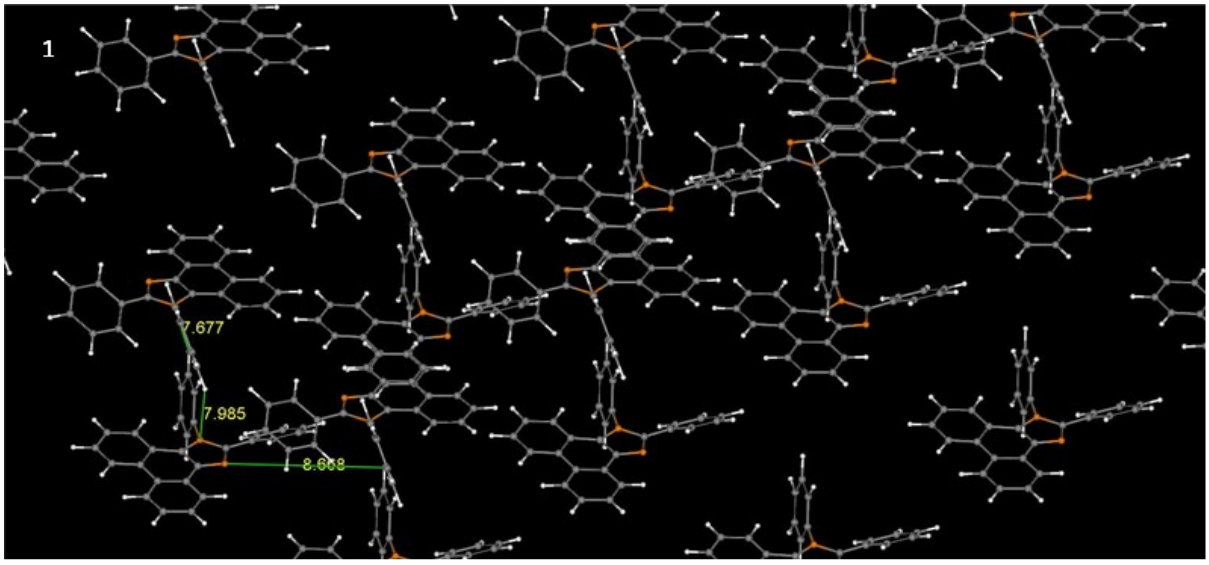

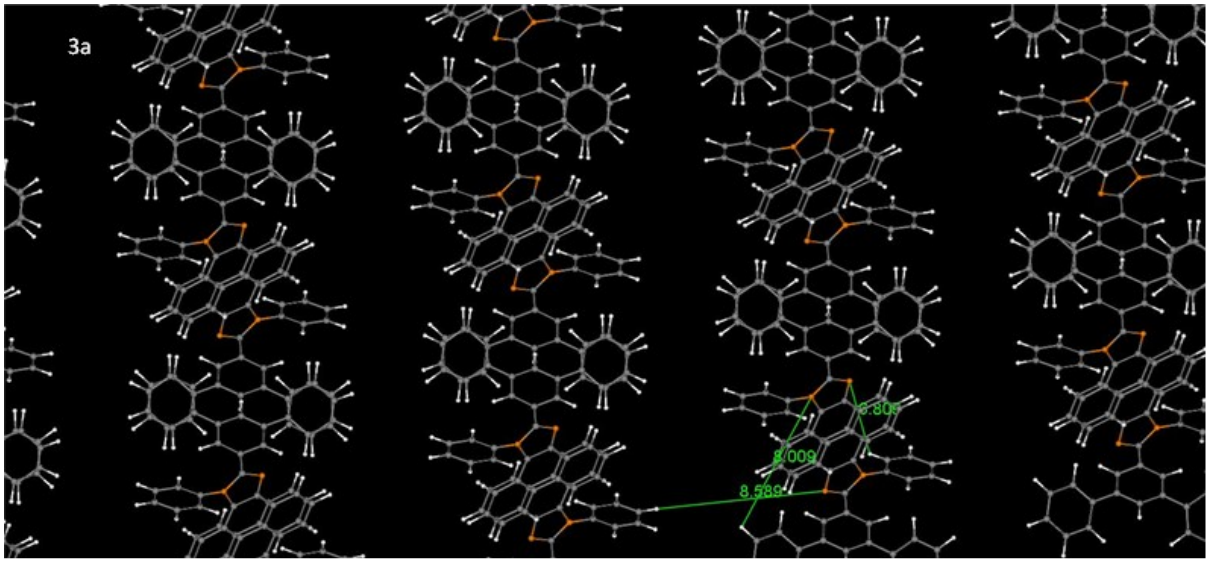
3a
3.804
8.009
8.589

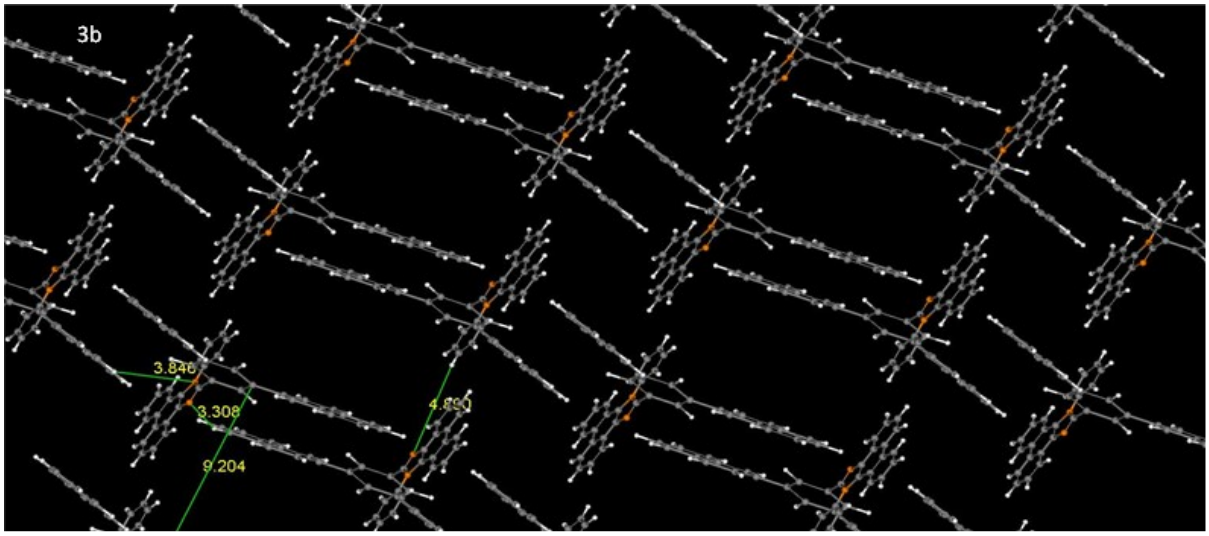
3b
3.846
3.308
9.204

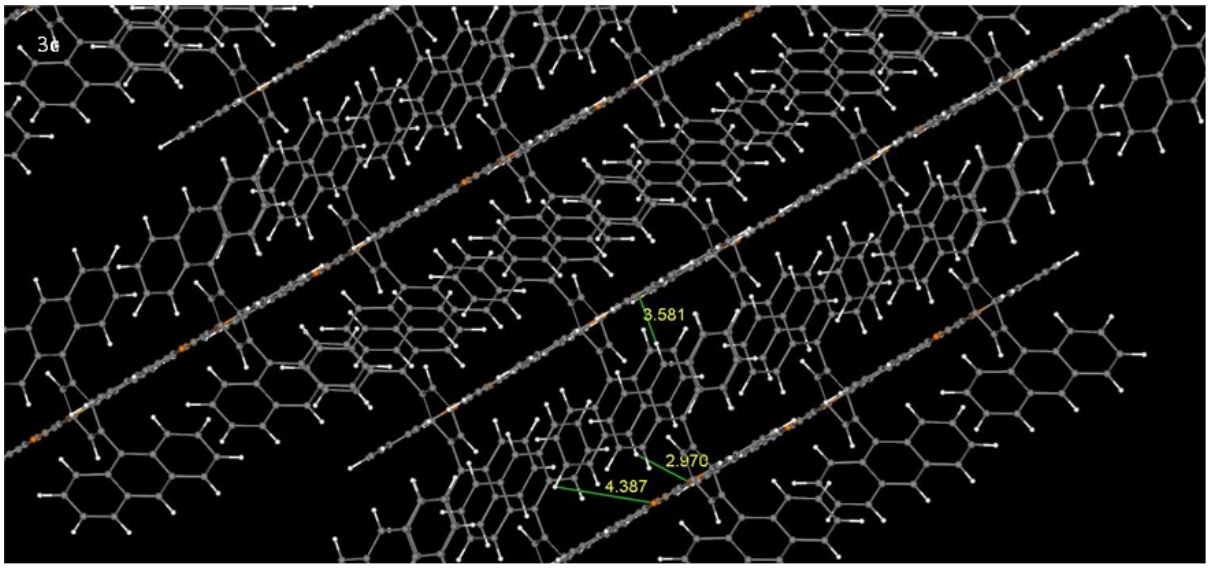
3c
3.581
2.970
4.387

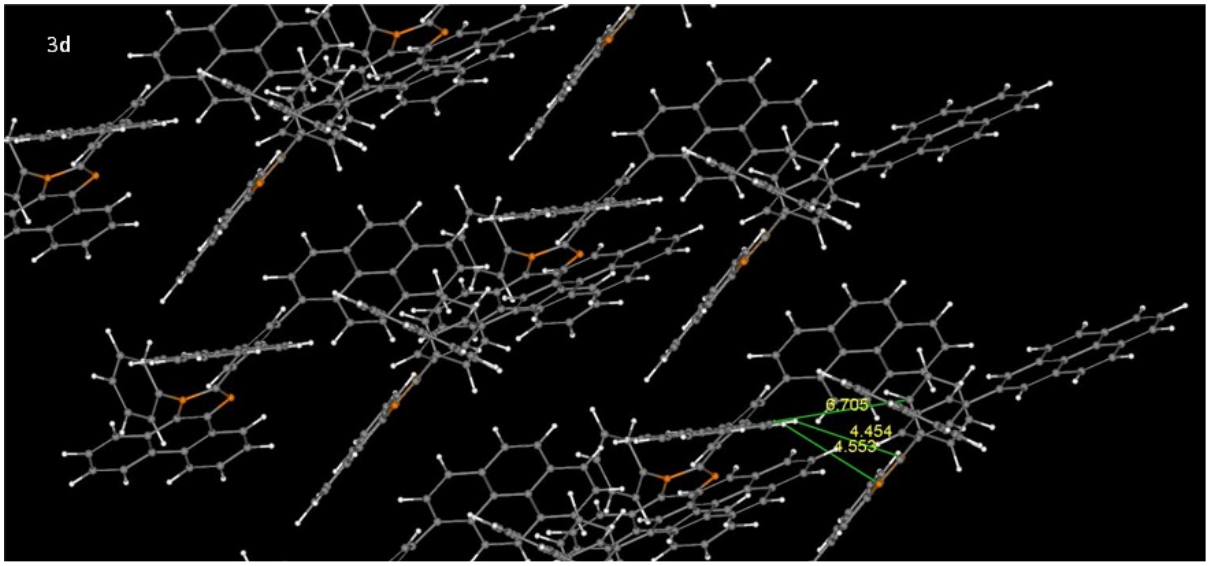

Figure S20. Molecular packing and hopping distance of the compounds **1, 3a-d**

Table S5. Crystalline parameters of the compounds **1, 3a-d**

Compounds	**Cell Parameters**	**Type of the Cell**	**Preferences**	**Symmetry**	**Hopping Distances** Å
1	16.2/13.1/8.23 90/90/90	Simple orthorhombic	4 3 1	P2	7.677 7.985 8.668
3a	18.4/15.9/9.48 90/90/90	Simple Orthorhombic	2 4 1	P-1	6.809 8.009 8.589
3b	16.1/20.7/18.5 90/90/90	Simple Orthorhombic	5 1 4	P21-C	3.308 3.846 4.890
3c	15.8/18.2/16.3 90/90/90	Simple Orthorhombic	3 2 3	P21-C	2.970 3.581 4.387
3d	21.1/20.9/10.4 90/90/90	Simple Orthorhombic	1 3 3	PC-B	4.454 4.553 6.705

The packing pattern was analyzed using different group symmetry elements, with only those configurations that met plausible parameter criteria and suitable hopping values being considered. Interatomic distances were determined based on volume and space group parameters, and all compounds exhibited a simple Orthorhombic geometry. The molecular packing of compounds **1, 3a-d** obtained by computational studies is depicted in

Figure S20. Compound **3c** showed the lowest hopping distances (2.970 Å, 3.581 Å, and 4.387 Å) among all five compounds due to the suitable arrangement of molecules. The hopping distance and the crystalline parameters of the compounds are given in **Table S5**, and the optimized geometry of compounds **1** and **3a-d** is depicted in **Figure S21**. The compound **3c** showed the least intermolecular distance of 2.970 Å, which shows a strong molecular crystal system and close packing of the molecules. Such a low intermolecular distance assists in promoting better charge transport properties in the molecular thin film.[6]

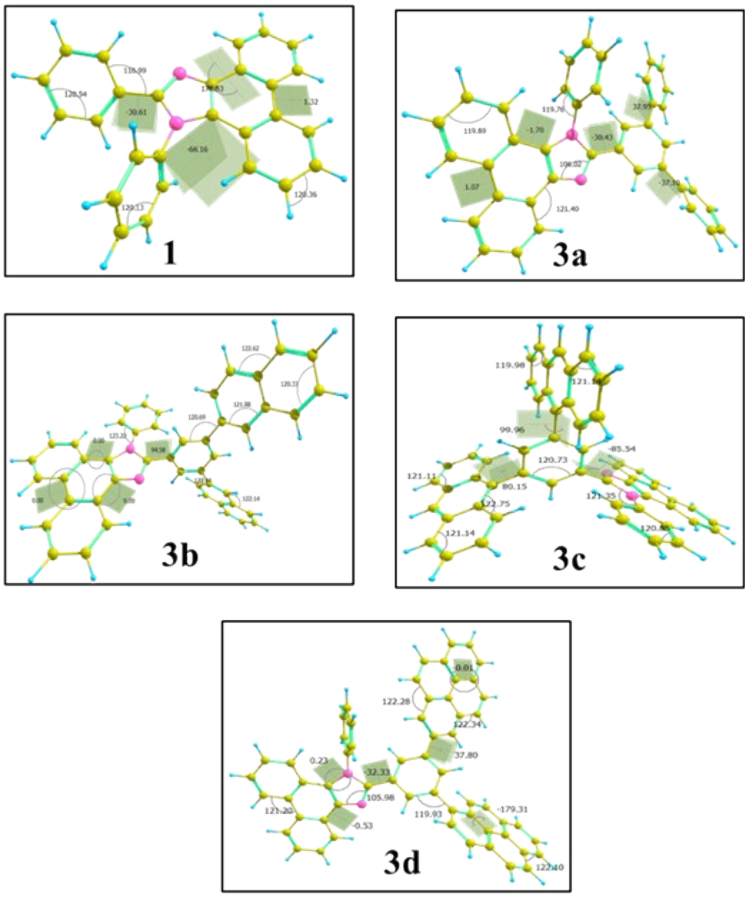

Figure S21. Optimized geometry of compounds **1, 3a-d**

References

(1) Jia, N.; Qi, S.; Tian, G.; Wang, X.; Wu, D. Tuning Electrical Memory Behavior from Nonvolatile to Volatile by Varying Tethering Positions of the Anthracene Moiety in Functional Polyimides. *J. Phys. Chem. C* 2016, **120 (46)**, 26217–26224.

(2) Sharma, B.; Thapa, A.; Sarkar, A. Ab-Initio Study of LD-HfO2, Al2O3, La2O3 and h-BN for Application as Dielectrics in MTJ Memory Device. *Superlattices Microstruct.* 2021, **150**, 106753.

(3) Akram, S. J.; Iqbal, J.; Ans, M.; El-Badry, Y. A.; Mehmood, R. F.; Khera, R. A. Designing of the Indacenodithiophene Core-Based Small Molecules for Optoelectronic Applications:

A DFT Approach. *Sol. Energy* 2022, **237**, 108–121.

(4) Kusama, H.; Orita, H.; Sugihara, H. TiO2 Band Shift by Nitrogen-Containing Heterocycles in Dye-Sensitized Solar Cells: A Periodic Density Functional Theory Study. *Langmuir* 2008, **24 (8)**, 4411–4419.

(5) Madsen, G. K. H.; Singh, D. J. BoltzTraP. A Code for Calculating Band-Structure Dependent Quantities. *Comput. Phys. Commun.* 2006, **175 (1)**, 67–71.

(6) Menzel, S.; Böttger, U.; Wimmer, M.; Salinga, M. Physics of the Switching Kinetics in Resistive Memories. *Adv. Funct. Mater.* 2015, **25 (40)**, 6306–6325.